ENERGY AND PARTICLE TRANSPORT MODELLING WITH A TIME DEPENDENT COMBINED CORE AND EDGE TRANSPORT CODE

The JET Team[1]
(presented by A. Taroni)

JET Joint Undertaking,
Abingdon, Oxfordshire,
United Kingdom.

Abstract

A new time dependent code has been developed by linking the $1^1/_2$ D core plasma transport code JETTO to the 2D edge plasma transport code EDGE2D/NIMBUS. The code includes a combined Bohm-gyro-Bohm type transport model for energy transport in the plasma core and this has been extended to include particle transport and a neoclassical transport barrier at the plasma edge for the simulation of JET hot ion H-modes. Outside the separatrix the transport coefficients extrapolated from the model are assumed to be constant. It is shown that the code gives a completely consistent time dependent simulation of the measured plasma profiles across the entire cross section of hot-ion ELM free discharges, including the scrape-off layer and divertor regions. The code also predicts that the ballooning stability limit is reached when a giant type I ELM appears in experiments.

1. INTRODUCTION

The importance of a global approach to transport studies, modelling simultaneously the entire plasma from the centre to the scrape-off layer (SOL) and divertor regions has been stressed recently by the development of transport models [1-2], relating the overall plasma performance to the behaviour of plasma in the boundary region.

As an example a model developed for the simulation of hot-ion H-mode plasmas in JET is considered. The model is based on the formation of a neoclassical transport barrier just inside the separatrix. The strength of the barrier depends on recycling. In the absence of accurate measurements of all the quantities relevant for an accurate evaluation of particle and energy sources and sinks just inside the separatrix, the assumptions made require to be validated by the proper modelling of experimental observations outside the separatrix.

At JET such a global approach to transport studies is now possible [3] thanks to the combination in a single code of the $1^1/_2$ D core plasma transport code JETTO and the 2D edge plasma transport code EDGE2D/NIMBUS, as described in section 2. The transport model presently used in the code is given in section 3, while in section 4 results of the simulation of a typical JET hot-ion H-mode are presented.

2. THE COMBINED CODE

The stand alone versions of the codes that have been combined into a global time dependent code are among the most advanced of their kind and are extensively used for the analysis and prediction of JET results. A link between JETTO and the impurity transport code SANCO, allowing a full multi-species

[1] See Appendix to IAEA-CN-64/O1-4, The JET Team (presented by J Jacquinot).

treatment of impurities in the plasma core, has recently been completed. Coupling between SANCO and the multi-species impurity package in EDGE2D/NIMBUS is in progress.

EDGE2D has been upgraded to include all components of the classical particle drifts in the equations and boundary conditions for all plasma species. Another recent upgrade of EDGE2D is the implementation of a 21 moment description of parallel transport. The transport coefficients are calculated using the reduced charge state (RCS) method [4], with no assumption on impurity density or atomic mass.

In linking the codes at a prescribed interface inside the separatrix continuity of densities and temperatures and of the corresponding total particle and energy fluxes at a chosen interface is enforced. This is achieved by imposing proper boundary conditions into each code at each time step. Poloidal averages of the quantities in EDGE2D/NIMBUS are used at the interface. Continuity of neutral profiles and fluxes is also enforced in order to have a consistent evaluation of particle sources.

An important point is that at the interface one code receives a variable or flux from the other and returns the corresponding flux or variable. This procedure ensures continuity of all relevant quantities with sufficient accuracy, even for fast transients, by simply running both codes with time steps typical of EDGE2D/NIMBUS, avoiding extra iterations at each time step. As a result the coupled code is very robust and requires less than 10% additional computer time with respect to the stand alone EDGE2D/NIMBUS code [3].

3. ENERGY AND PARTICLE TRANSPORT MODELS

The transport models used in the code are mainly empirical. Their derivation and justification can be found in [5].

The transport model for energy is a combination of Bohm and gyro-Bohm-like terms. The corresponding thermal conductivities are:

$$\chi_e = \chi_B + \chi_{gB}$$
$$\chi_i = 2\chi_B + \chi_{gB} + \chi_{neo,i} \qquad \text{for} \quad 0<r<r_I$$

The model includes a region of finite width at the plasma edge from a radius r_I to the plasma boundary $r=a$ ($\rho_I<\rho<1$ in a normalised radial flux surface co-ordinate) where transport is close to neoclassical. A neoclassical barrier for impurity transport in JET ELM free H-mode discharges was previously considered in the SANCO code [6] and taken into account as a boundary condition of the energy equations in JETTO [1].

The Bohm and gyro-Bohm parts of the model, used for $\rho< \rho_I$, are given by:

$$\chi_{gB} = c_{gB}\sqrt{T_e}\,\frac{\nabla T_e}{B_T^2}$$

$$\chi_B = c_B\,\frac{\nabla P_e}{nB_T}\,q^2 a^2 L_{T1}^{-1}$$

where to compute the average of the inverse of the characteristic length of the temperature variation:

$$L_{T1}^{-1} \equiv < \nabla T_e/T_e >_{0.8<\rho<\rho_1}$$

the first order approximation is taken: $L_{T1}^{-1} \sim \left(T_{e,\rho=0.8} - T_{e,\rho=\rho_1}\right)/T_{e,\rho=\rho_1}$. c_{gB} and c_B have been chosen by calibrating the model in a number of JET L-mode discharges and are kept constant [1].

The Bohm-like term is non local, via its dependence upon L_{T1}^{-1}. This dependence allows the use of the model in both H- and L-mode, by reducing the Bohm-like term in H-mode. In L-mode the transport barrier is switched off.

In the same region particle transport is given by an effective diffusion coefficient:

$$D_{eff} = \alpha_D(r)\frac{\bar{\chi}}{\langle n_e \rangle} \text{ with: } \bar{\chi} = \frac{\chi_e \chi_i}{\chi_e + \chi_i}$$

where $<n_e>$ is the volume average density and $\alpha_D(r)$ is a shape factor (including a normalising constant density) that reduces D_{eff} with respect to χ as ρ increases (Fig.1). Such an empirical dependence of D_{eff} seems to be required to match at the same time:

a) the experimental density profiles;
b) the neutral fluxes computed by EDGE2D (which match experimental values of D_α emission); and
c) the lack of strong variation with time of the ion saturation current density at the divertor targets in low recycling ohmic and hot ion H-mode discharges.

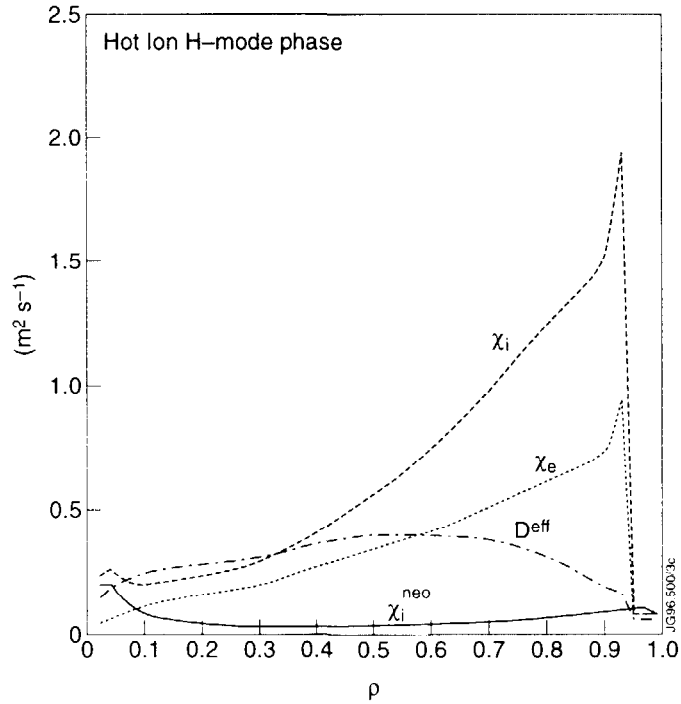

Fig.1 Radial dependence of the transport coefficients in the hot ion H-mode.

The shaping factor $\alpha_D(r)$ and the inverse dependence upon $<n>$ are to be considered as an indication of the existence of an inward particle pinch velocity term increasing strongly towards the boundary and increasing with density. Work is in progress to include explicitly such a term in the model.

In the present version of the code the width of the neoclassical boundary transport barrier $\Delta = a - r_l$ is imposed and kept constant in time. Typically $\Delta \approx 5$ *cm*,

which for the JET hot ion H-modes with plasma current $I \approx 3$ *MA* simulated so far corresponds to a few ion banana orbit radii ρ_b. The main effect of the barrier is to act as a 'plug' which at low collisionality provides thermal fluxes essentially independent of temperature but directly proportional to $n^2 Z_{eff}$ [1]. Such plugging is obtained by assuming within the barrier region:

$$\chi_i = \chi_e = D \propto \frac{\Delta}{\rho_b} \chi_i^{neo}$$

where χ_i^{neo} is the neoclassical ion thermal diffusivity. This corresponds in first approximation to assuming $\chi_i = \chi_e = D_{eff} \approx \chi_i^{neo}$ and $\Delta \propto \rho_b$.

For the simulations shown in the next section, the transport coefficients in the SOL region are assumed to be the same as the transport coefficients computed at the JETTO/EDGE2D interface (≈ 2 *mm* inside the separatrix) from the core transport model. However better agreement with measurements in the divertor region is obtained by including an explicit inward pinch velocity term $V \approx 15\ D/a$ in the SOL particle flux (even if the particle diffusion coefficient is rather small as shown in Fig.1).

4. SIMULATION OF HOT ION H-MODES

The hot ion H-mode is a very interesting plasma regime in JET, and has provided record values of energy confinement and fusion reaction rate. This regime is usually entered directly from a low recycling ohmic regime following the formation of the separatrix X-point, soon after ($\approx 100\text{-}150$*ms*) the application of vigorous neutral beam injection (NBI) heating. The good, ELM-free, confinement phase is characterised by an almost linear increase of the energy content lasting for about one second, and usually terminates as a result of some MHD activity (sawtooth, giant type I ELM, "outer" mode) [7]. These pulses have been extensively studied by means of the JET transport codes. In the following results will be presented of the simulation of a typical representative of these pulses, the *3MA, 3.4T* Pulse Number 32919 obtained with the Mark I divertor configuration.

The simulation has been carried out assuming a pure plasma but including Z_{eff} and impurity radiation from the experimental data base. NBI power deposition profiles computed by the TRANSP code as a function of time have been used, assuming that the injected particles (and corresponding energy) lost via shine-through and direct charge exchange losses at the plasma periphery are promptly lost at the vessel wall. This assumption might have to be reviewed, if necessary,when an accurate experimental evaluation of the SOL power balance will becomes available.

The results presented here refer mainly to the time evolution of the discharge from the ohmic phase ($11.6\text{s-}12\text{s}$) into the ELM-free high performance phase ($t < 13s$). Some results for the so called roll-over phase preceding a giant ELM at $t \approx 13.3s$ will also be briefly referred to. The transition to H-mode is simulated by switching on the neoclassical boundary barrier $0.125s$ after NBI is switched on at $t \approx 12.0s$. The benign ELMs at the beginning of the H-mode are ignored (Fig.2).

The density decrease during the ohmic phase is simulated by assuming that the target recycling coefficient R_t is less than unity during this phase (see Table I, showing typical values of the quantities that characterise particle recycling during the ohmic and H-mode phases). The rate of increase of the total plasma particle content dN/dt during the NBI phase exceeds the NBI fuelling source S_n^{NBI}. The extra influx of neutrals Φ_0^{ex} necessary to simulate the plasma density increase, without any external puff being activated, has been assumed to be released

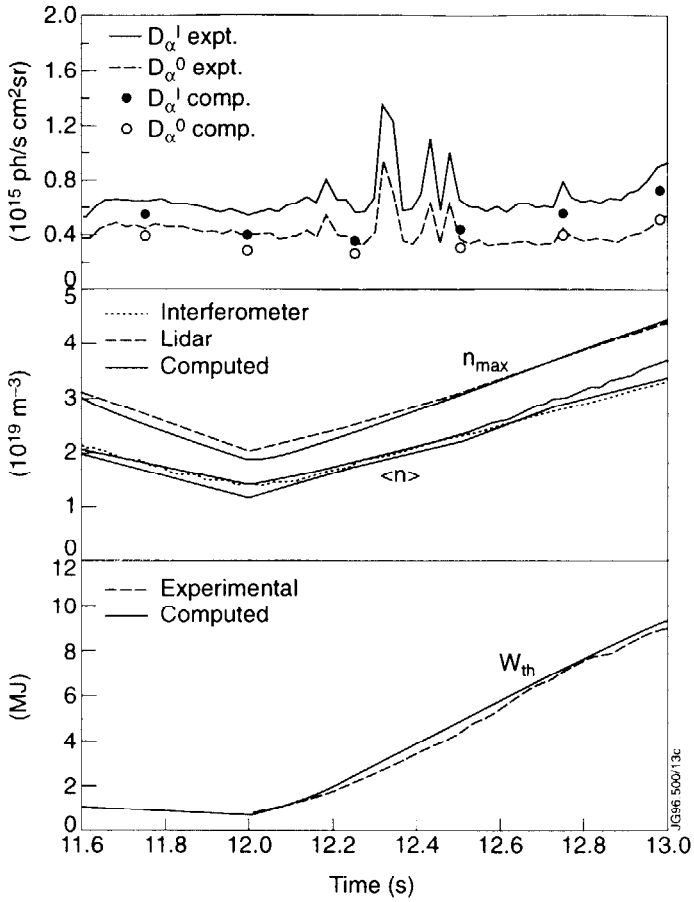

Fig.2 Experimental and computed time evolution of D_α emissivities (see text), averaged and peak core plasma densities, and thermal energy content.

Table I

	dN/dt	S_n^{NBI}	F_0^{ex}	F_0^c	F_i^c	F_i^t	F_0^{pump}	F_0^{leak}	R_t
OH	*-1.35*	*0.0*	*0.0*	*3.3*	*4.65*	*30*	*0.14*	*0.4*	*0.96*
H	*1.75*	*1.4*	*0.5*	*3.2*	*2.85*	*30*	*0.15*	*0.5*	*1.0*

from the divertor or from different regions along the vessel walls without significant variations of the computed core plasma performance. The numerical results shown in this paper refer to divertor release. Table I shows for comparison also values, computed by the code, of the influx of neutrals into the core Φ_0^c, the outflux of ions from the core Φ_i^c, the total flux of ions to the target Φ_i^t, the pumped flux of neutrals Φ_0^{pump} and the flux of neutrals through the bypass leaks [8] in the sub-divertor region Φ_0^{leak}. Units are 10^{21} s^{-1}.

The temporal evolution of the computed and experimental averaged and peak core plasma density in the ohmic and H-regime is shown in Fig.2. The same figure compares the evolution of the D_α emission integrated along lines of view looking at the inner (D_α^I) and outer (D_α^O) divertor plates, and of the thermal energy content.

Figure 2 indicates, in particular, that the distribution of neutrals in the SOL and divertor regions, their influx into the plasma core, and the particle transport in both regions are all consistent with experimental observations. The resulting charge exchange loss terms computed by the code reach a maximum in excess of *2.5 MW* at *t≈13 s*. Their profiles are strongly peaked at the separatrix being negligible at the plasma centre.

Figure 3 compares experimental and computed profiles of the ion saturation current density in the ohmic and H-mode phases, showing little variation of this quantity, consistent with recycling being very low in both phases.

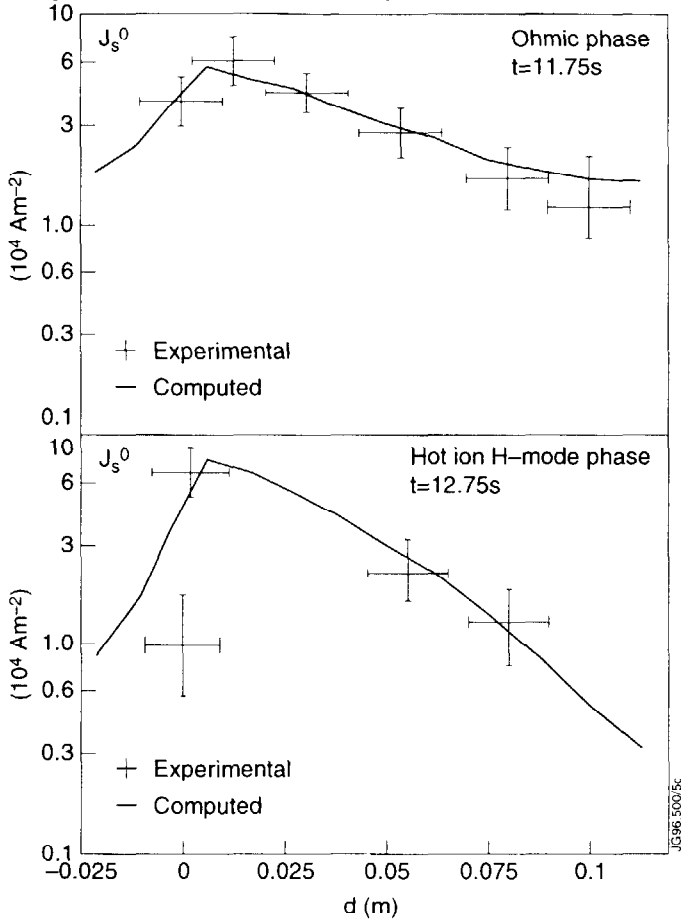

Fig.3 Computed and experimental spatial variation of the ion saturation current density at the outer target as a function of distance from the separatrix.

The simulated and predicted evolution of the ion temperature and of the total neutron rate is given in Fig.4. It can be seen that a natural saturation of the ion temperature is predicted by the model as a consequence of the density increase. It can also be seen that the model somewhat underestimates the central ion temperature towards the end of the good performance phase, while the neutron rate is slightly overestimated. This seems to indicate a small inconsistency in the experimental data, which is confirmed by TRANSP analysis of this kind of pulse.

A number of code runs have been dedicated to the simulation of the roll-over phase by increasing the core fuelling from the SOL and Z_{eff} before the roll-over takes place. While some features of the roll-over, such as the saturation of the energy content, are correctly represented in these simulations, others are not. For

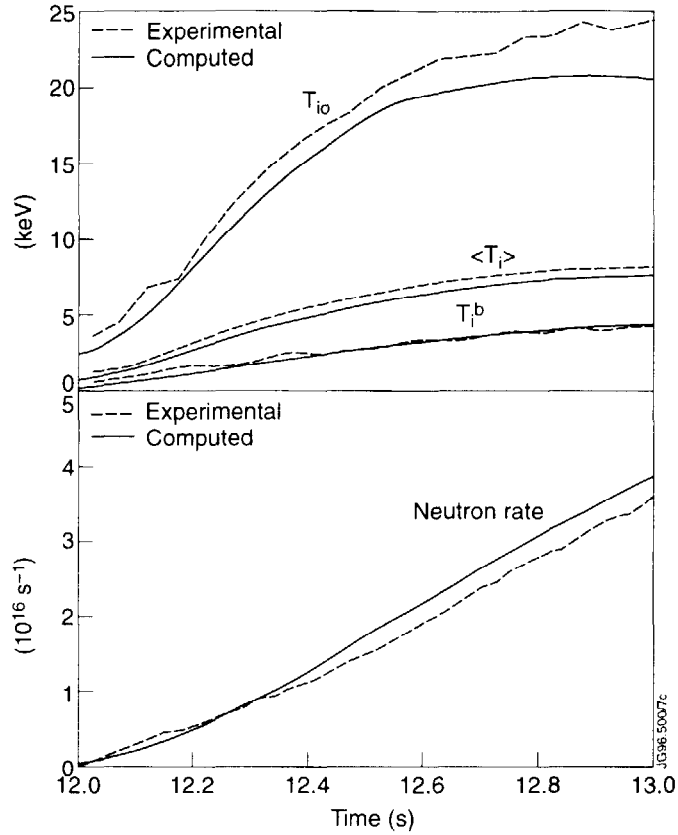

Fig.4 Experimental and computed time evolution of the ion temperature at the plasma centre and at the top of the transport barrier. The average ion temperature and the neutron rate are also shown.

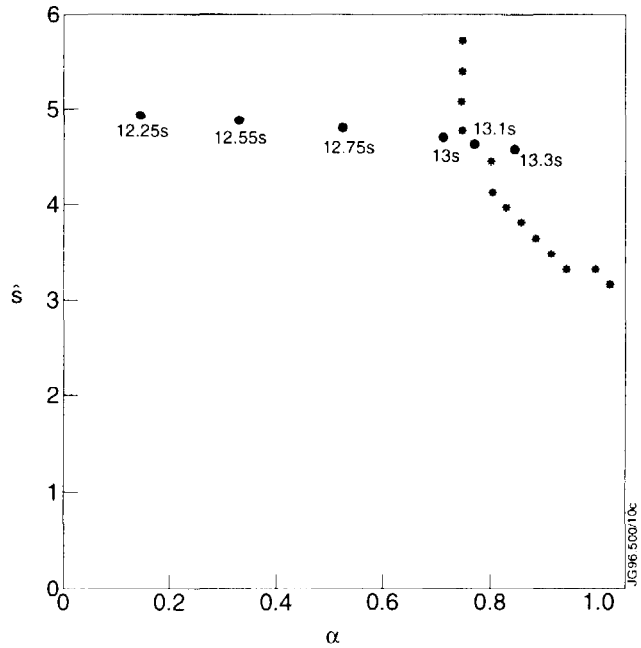

Fig.5 Trajectory of the discharge in the ballooning stability diagram of s (the normalised shear) versus α (the normalised pressure gradient).

example, the predicted decrease of the central ion temperature is generally underestimated while the increase in the ion saturation current is overestimated. Clearly more work is required for a complete modelling of the roll-over phase.

An interesting result is found by computing at the core plasma boundary the trajectory of the discharge in the ballooning stability diagram. This is done using the simulated plasma profiles in the IDBALL package [9] linked to the combined code. This trajectory approaches and hits the stability limit at approximately the time when first a roll-over, that practically does not modify the neoclassical transport barrier ($t \approx 13.1$), and then a giant ELM that strongly reduces it ($t \approx 13.3$), take place (Fig.5).

5. CONCLUSION

The combined code for core and edge transport studies developed at JET, together with the availability of measurements in the two regions is a powerful tool to simulate tokamak discharges in a time dependent way.

By eliminating ad hoc (and sometimes convenient) assumptions at the interface between core and boundary region this code provides a very tough and complete test for transport models, including the effect on the SOL of transport assumptions in the core and vice versa. Results from the combined code can be used to improve modelling in the stand alone core and edge transport codes.

The transport model used in the code, although not fully predictive and essentially empirical, has proven to be useful to clarify some important aspects of the evolution of hot-ion H-modes. In particular it supports the hypothesis that type I giant ELMs might be caused by ballooning instability in the edge transport barrier region.

ACKNOWLEDGEMENTS

Particularly grateful acknowledgement is due to the following for their contribution in developing the code and the transport models, for discussion of the results, and for providing experimental information:

B.Balet, A.V.Chankin, A.Cherubini, G.Corrigan, M.Erba, M.Fichtmueller, H.Guo, L.Lauro-Taroni, G.K.McCormick, V.V.Parail, G.Radford, R.Simonini, J.Spence, E.Springmann.

REFERENCES

[1] CHERUBINI, A., et al., Plasma Phys. Control. Fus. **38** (1996) 1421-1425.
[2] KOTSCHENREUTHER M., et al., Phys. Plasmas **2** (1995) 2381.
[3] TARONI, A., et al., to appear in Controlled Fusion and Plasma Physics (Proc. 23rd Eur. Conf. Kiev, 1996).
[4] BOLEY, C.D., et al., Phys. Fluids **22** (1979) 1280.
[5] ERBA, M., et al., to appear in Plasma Phys. Control. Fus.
[6] LAURO-TARONI, L., et al., in Controlled Fusion and Plasma Physics (Proc. 17th Eur. Conf. Amsterdam, 1990), Vol. 14B, Part I, European Physical Society, Geneva (1990) 247.
[7] THE JET TEAM (presented by P. J. Lomas), IAEA-CN-64/A1-5, this Conference.
[8] THE JET TEAM (presented by G. C. Vlases), IAEA-CN-64/A4-1, this Conference.
[9] HENDER, T., private communication.

OPTIMISATION OF JET PLASMAS WITH CURRENT PROFILE CONTROL

The JET Team[1]
(Presented by C Gormezano)

JET Joint Undertaking,
Abingdon, Oxfordshire,
United Kingdom.

Abstract

Internal transport barriers extending up to r/a = 0.55 have been achieved on JET by tailoring the plasma current profile by proper current ramps up to 3MA, with or without heating. The best performing discharges are produced when a long L-mode phase with high core confinement can develop before the onset of an H-mode. High central ion temperatures (32keV) and electron temperatures (15keV) are simultaneously produced resulting in neutron rates comparable to the best Hot Ion H-mode in JET with a time duration (0.5s) in excess of the energy confinement time.

1. INTRODUCTION

Operating a tokamak with higher confinement than predicted by the usual confinement scaling laws [1] has several advantages. One of them is to increase the fusion yield for a given input power allowing access in JET to regimes in DT operation where the alpha power can play a significant role. Another advantage is to operate a fusion reactor at lower plasma current. This opens the possibility of steady state operation, especially at high poloidal beta, high bootstrap current, by reducing the demand on non-inductive current drive. These so-called advanced tokamak scenarios require the demonstration of improved confinement not only transiently but for long duration.

Current profile control has proved to be an important technique to optimise confinement of tokamak plasmas. For example, in JET, current profile modification has produced high confinement with a reversed shear magnetic configuration in the pellet enhanced H-mode (PEP + H-mode) [2] and also in high β_p, high bootstrap current plasmas [3]. Ion minority current drive has been used to stabilise or destabilise sawteeth by local modifications of the current profile [4]. Lower Hybrid Current Drive (LHCD) has been used to modify the current profile before the formation of a Hot Ion H-mode [5], to raise the safety factor on axis q(o) above unity and provide sawtooth suppression during the high power heating phase resulting in an increase of the overall neutron rate. This technique has also allowed the addition of Ion Cyclotron Resonance Heating (ICRH) and Neutral Beam Injection (NBI) at high power levels in the Hot Ion H-mode which, in the absence of sawteeth, benefits from increased power deposition in the plasma core and a 30% increase in confinement [6].

Large efforts have been made to develop discharges with reversed shear either by using LHCD (Tore Supra) [7] achieving high confinement quasi steady-state discharges or by making use of heating in the current ramp phase to freeze

[1] See Appendix to IAEA-CN-64/O1-4. The JET Team (presented by J Jacquinot), with the collaboration of the DIII-D Team.

the current profile to achieve an optimised q profile resulting in good central confinement [8-10].

In current ramp experiments in JET in the 1994/95 campaign, a few MW of LHCD power was applied during a fast current ramp (1MA/s). A substantial increase of the electron temperature (up to 10keV) was observed during the initial phase of the reversed shear. Transport analysis has shown that the electron thermal diffusivity during this phase was reduced by one order of magnitude to values close to the level of the neo-classical thermal conductivity. This phase of enhanced confinement was not maintained when heavy gas puffing was used to raise the density in order to allow NBI with low shine-through. A broad density profile resulted and an ELMy H-mode was produced with 12MW of NBI power.

New hardware has allowed operation of the JET NBI system at lower density. With proper current ramp and power waveforms, large Internal Transport Barriers (ITB) have been obtained with a combination of NBI and of ICRF resulting in high performance plasmas.

2. INTERNAL TRANSPORT BARRIER

In JET, the ITB is established when the main power waveform is applied during the current ramp phase of the plasma, with or without a preheating phase. The main evidence of an internal barrier can be seen from the evolution of the ion temperature profile as shown in Figs.1 and 2 for two different timings of the power application. With early power application (Fig.1), a barrier is formed very close to the plasma core, about 1.2 s after the start of the heating. This barrier then moves outwards to r/a = 0.45. The discharge remains in an L-mode during the whole development of the ITB and is generally terminated by a disruption, following high frequency core MHD.

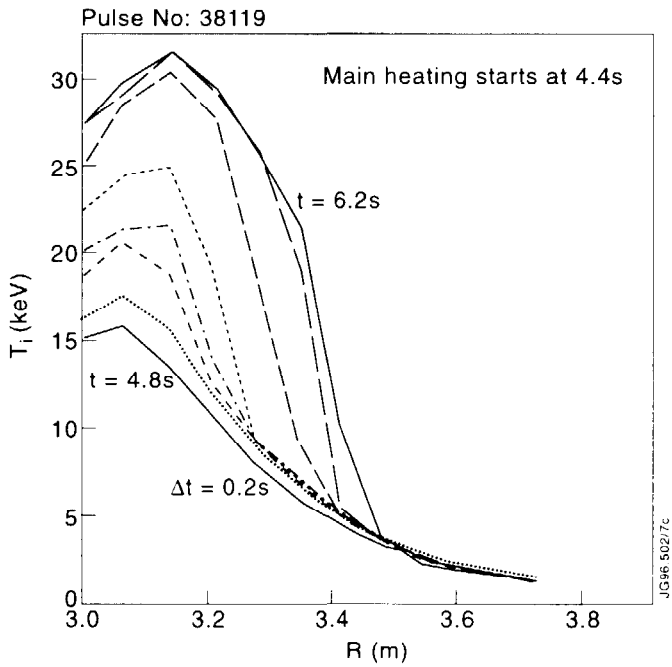

Fig.1 Evolution of ion temperature profile from charge exchange recombination (B_t = 3.4T; 2.5 < I_p < 3MA) with early power waveform and 1MW (ICRH) of preheating.

ITBs have also been established when power is applied later in time and with no preheating as shown in Fig.2. The barrier is established almost immediately with a slow expansion up to r/a ~ 0.55. In this case, the L-mode

phase is followed by an H-mode with central pressure up to 2.5 bar. It can be noted that a pedestal is formed at the plasma periphery and the whole ion temperature profile is raised by about 2 keV. These profiles are quite different from profiles of equivalent Hot Ion H-modes with similar power and neutron yield which shows significantly lower central temperature and much higher edge temperature. Similar transport barriers can be seen on the electron temperature profiles and to a lesser extent on the density profiles.

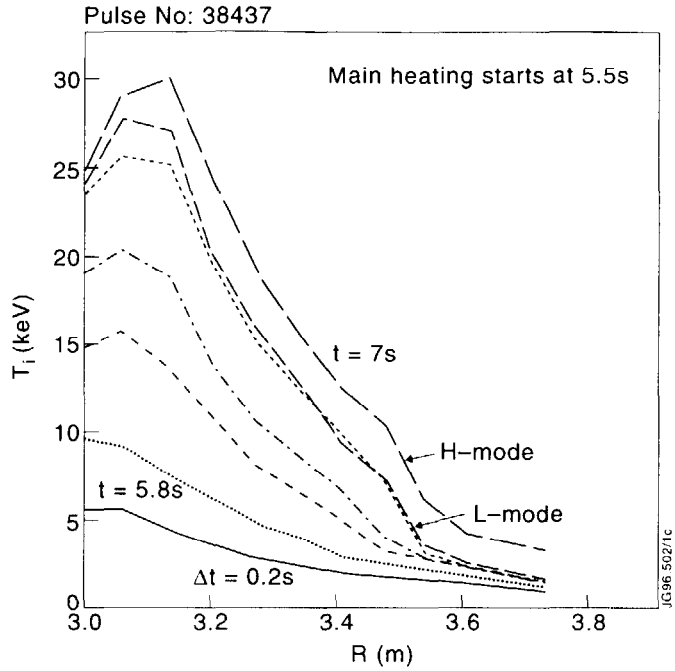

Fig.2 Evolution of ion temperature profile from charge exchange recombination (B_t = 3.4T; 2.5<I_p < 3MA) with late power waveform and no preheat.

ITBs are very sensitive to the timing of the high power waveform as illustrated in Fig.3. The ramp rate of the discharge to 2.5MA is adjusted to the highest rate compatible with the absence of MHD activity during the ramp. The second ramp in current is used to delay the onset of the H-mode. If H-modes appear too early, the L-mode peaked pressure profile is not yet fully established and NBI penetration is compromised by the formation of the edge pedestal. In addition, the strike points of the last closed surface are maintained close to the divertor pump entrance to prevent the edge density from forming quickly. This also delays the onset of the H-mode. The present configuration has low triangularity due to the mode of operation used for this campaign. As shown in Fig.4, early heating results in a late core transition. Late heating leads to an early H-mode which prevents the establishment of an ITB. The best performance (without disruption) has been obtained when the power is applied 5.5 s after the beginning of the discharge. Note that discharges with an ELMy H-mode obtained with late heating still have peaked density profiles because q(o) remains above unity and sawteeth are absent. The neutron yield is about 2 times higher than corresponding sawteething discharges with similar power. An optimisation of this mode of operation for high performance steady operation is still outstanding.

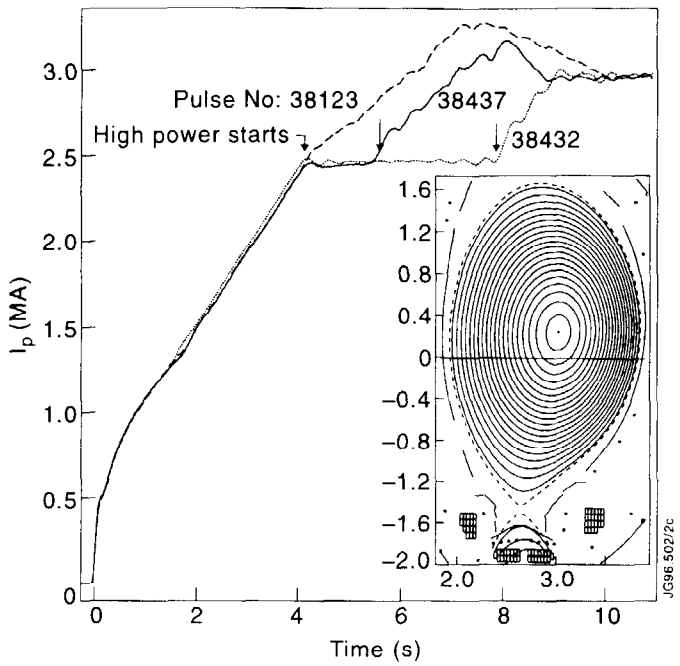

Fig.3 Typical current waveforms and flux contours for ITB. In the absence of heating, sawteeth appear at about t = 9 s.

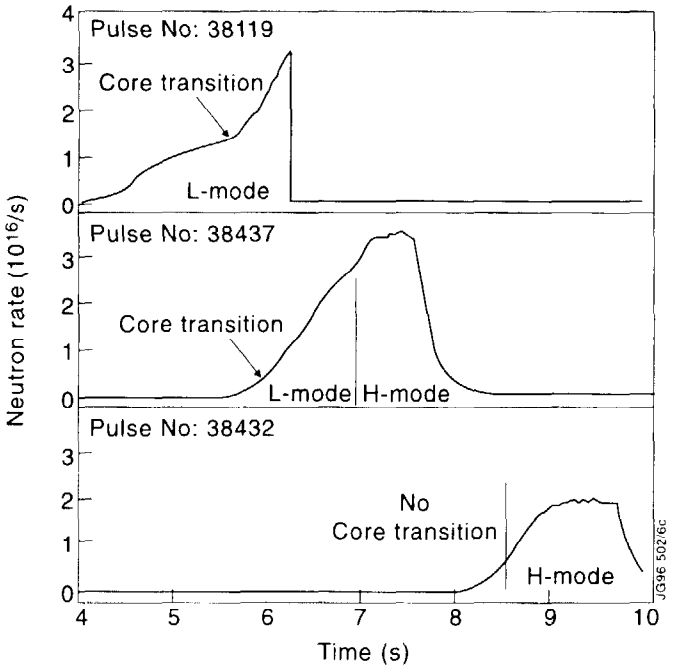

Fig.4 Time evolution of the neutron yield for different timing of the power waveform with a total power of 25MW. No ITB is observed when power is injected after 6 s from the start of the discharge.

3. HIGH PERFORMANCE DISCHARGES WITH SHEAR OPTIMISATION

An example of a high performance discharge where the L-mode phase is followed by an H-mode is shown in Fig.5. The H_{89} factor reaches 2 during the L-mode phase and 2.5 during the H-mode phase. These discharges have about 30% less stored energy than a comparable Hot Ion H-mode but a similar neutron yield because of the peaked profiles. There is no evidence of impurity accumulation on this time scale, Z_{eff} remaining constant at about 1.7. It is to be noted that in the case shown in Fig.5 the neutron yield remains about constant during the ELMs for as long as the power was applied, i.e. for times longer than the energy confinement time (0.4 s). However, in similar pulses a giant ELM often leads to a degradation of performance. The largest neutron yield which has been achieved in such discharges equals the highest yield in the Hot Ion H-mode achieved on JET in the present campaign.

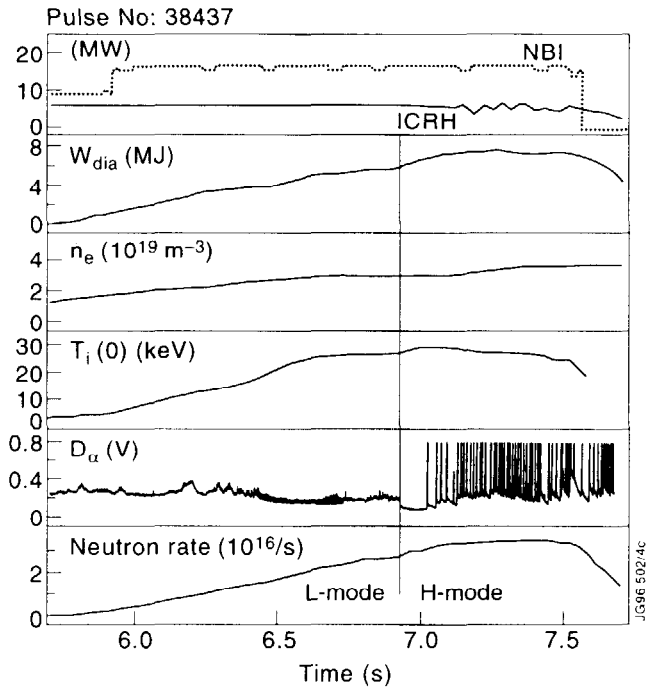

Fig.5 Time history of a high fusion yield pulse with shear optimisation (B_t = 3.4T; 2.5 < I_p 3MA). ICRH frequency (51MHz) corresponds to a resonance (H minority or 2nd harmonic D) close to the centre.

Several experimental observations (such as: no significant flux of gamma radiation, an increase of only 2 to 3 keV in electron temperature when comparing NBI only and combined heating shear optimised discharges), together with numerical simulations indicate that a substantial part of the Ion Cyclotron wave is coupled to fast deuterons at energies lower than a few hundred keV leading to ion heating, especially at high electron temperature.

In the absence of a proper simulation of the damping and heating of the Ion Cyclotron wave in such plasmas, a TRANSP simulation has been made for a discharge with shear optimisation where the ICRH power was off for 1 s. As shown in Fig.6, good agreement between experimental values and simulation is obtained with a significant thermal yield reaching more than 50% of the total yield. The current profile in JET can only be measured through a combination of polarimetry and magnetic measurements to reconstruct the equilibrium (EFIT).

Unfortunately, only one polarimeter channel can reasonably be used. Consistency checks have been made between the equilibrium reconstruction and the calculated current profile in TRANSP. It is not yet possible to have a reliable q profile, but it appears that a strong reversed shear is not necessary to trigger an ITB, in agreement with observations on DIII-D. The location of the barrier at the onset of the H-mode appears to be in the vicinity of a q=2 surface.

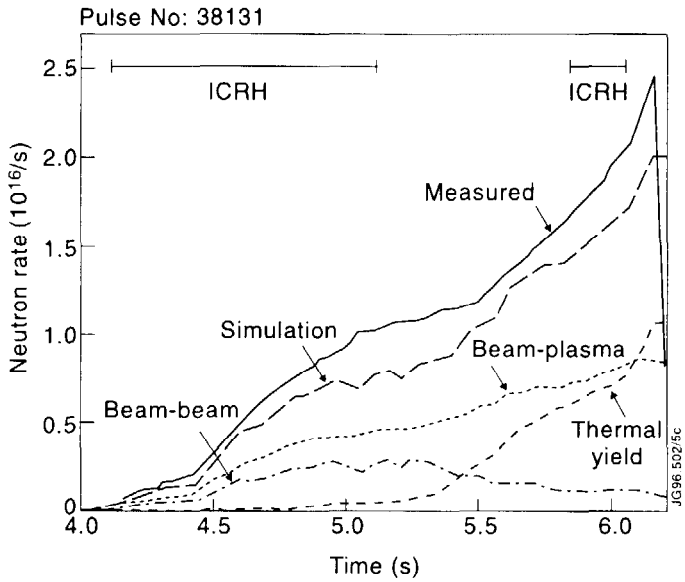

Fig.6 TRANSP simulation of pulse 38131. NBI (14MW) is on from 4 s ICRH (7MW) is off for 1 s.

4. POWER DEPENDENCE AND LIMITATIONS

A minimum power is required to obtain ITB in JET, as shown in Fig.7 where the data base of neutron rate versus total injected power is given for all discharges where a sustained core transition has been achieved. A substantial part of the data scattering is due to the large range of power, density and configuration waveforms investigated for shear optimisation, in particular neutron rate is very sensitive to target density. The low range of power corresponds to power step-down experiments, similar to Fig.6, where 6 to 8MW of ICRH power was switched off after about 1s when an ITB was already established. The dependence of this minimum power versus various parameters such as magnetic field and plasma current has not been done yet. The performance during the L-mode phase was often limited by low frequency, n =1 modes hardly rotating, sometimes locked, located near the q = 2 surface. These modes are very different from the modes appearing during pulses with early heating with an n = 1 structure rotating at very high frequency and leading to a disruption. The low frequency modes shown in Fig.8 are not disruptive, but limit the increase of neutron yield especially when these modes are locked. Their amplitude is variable which contributes to the scatter in the data and their dependence on plasma parameters is under investigation.

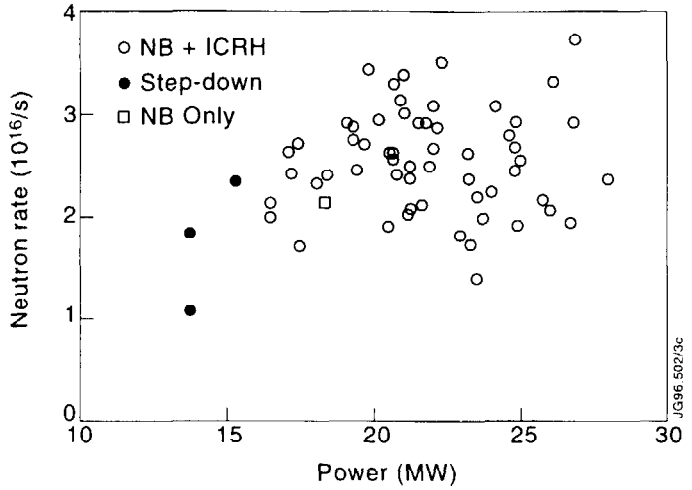

Fig.7 Neutron rate versus power for discharges with sustained core transitions .

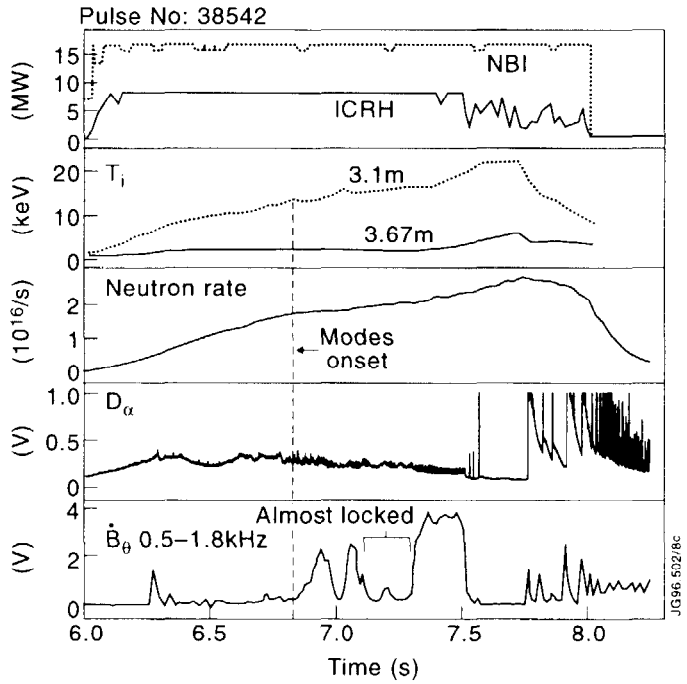

Fig.8 Time history of a discharge where low frequency MHD limits L-mode performance.

5. SUMMARY AND CONCLUSIONS

Internal Transport Barriers have been obtained on JET in low triangularity discharges with shear optimisation. The best performing discharges have a long L-mode phase followed by an H-mode phase which is deliberately delayed by a second current ramp. Up to 28MW of combined power has been used for discharges with I_p from 2.5 to 3MA and B_t = 3.4T with low target density. Internal barriers with r/a = 0.55 have been achieved, resulting in:

- high confinement L-modes (H_{89} = 2)
- simultaneous high T_i (32keV) and T_e (15keV)

- an ITB is only formed above a power level of about 17MW in these conditions
- high neutron yield (3.9 10^{16}/s) comparable to the best Hot Ion H-modes for times longer than an energy confinement time
- no apparent accumulation of impurities
- a high ratio of neutron yield to stored energy.

It should be noted that these are still early experiments. More development, including optimisation of pre-heat techniques, use of non-inductive current drive (LHCD and phased ICRH), use of higher triangularity, together with further optimisation of the ELMy H-mode phase, might lead to higher performance and/or extended duration. Extending the duration of the high performance phase is of obvious importance for reactor application.

6. REFERENCES AND ACKNOWLEDGEMENTS

[1] THE JET TEAM (presented by J.G. Cordey), IAEA-CN-64/AP1-2 this conference.
[2] TUBBING, B., et al., Nucl. Fusion, **31** (1991) 839.
[3] CHALLIS, C., et al., Nucl. Fusion, **33** (1993) 1097.
[4] BHATNAGAR, V.P., et al., Nucl. Fusion, **34** (1994) 1579.
[5] EKEDAHL, A., et al., to appear in Controlled Fusion and Plasma Physics (Proc. 23rd Eur. Conf. Kiev, 1996).
[6] COTTRELL, G., et al., ibid.
[7] LITAUDON, X., et al., ibid.
[8] JET TEAM (presented by C. Gormezano), in Plasma Physics and Controlled Nuclear Fusion Research (1994) (Proc. 15th Int. Conf. Seville, 1994) Vol. 1, IAEA, Vienna (1996) 633.
[9] LEVINGTON, F.M., et al., Phys. Rev. Letters (1995) 417.
[10] STRAIT, E.J., et al., Phys. Rev. Letters (1995) 4421.

Specific contributions from C Greenfield, E Lazarus, T Luce, B Rice, E Strait (GA), M Zarnstorff, G Schmidt (PPPL) and from B Lloyd, C Warwick, and C Hunt are gratefully acknowledged.